Let-7b-5p in vesicles secreted by human airway cells reduces biofilm formation and increases antibiotic sensitivity of *P. aeruginosa*

Katja Koeppen[a,1], Amanda Nymon[a], Roxanna Barnaby[a], Laura Bashor[a], Zhongyou Li[a], Thomas H. Hampton[a], Amanda E. Liefeld[a], Fred W. Kolling[b], Ian S. LaCroix[b], Scott A. Gerber[b], Deborah A. Hogan[a], Swetha Kasetty[c], Carey D. Nadell[c], and Bruce A. Stanton[a]

[a]Department of Microbiology and Immunology, Geisel School of Medicine at Dartmouth, Hanover, NH 03755; [b]Norris Cotton Cancer Center, Geisel School of Medicine at Dartmouth, Lebanon, NH 03756; and [c]Department of Biological Sciences, Dartmouth College, Hanover, NH 03755

Edited by Dianne K. Newman, California Institute of Technology, Pasadena, CA, and approved June 3, 2021 (received for review March 25, 2021)

Pseudomonas aeruginosa **is an opportunistic pathogen that forms antibiotic-resistant biofilms, which facilitate chronic infections in immunocompromised hosts. We have previously shown that *P. aeruginosa* secretes outer-membrane vesicles that deliver a small RNA to human airway epithelial cells (AECs), in which it suppresses the innate immune response. Here, we demonstrate that interdomain communication through small RNA–containing membrane vesicles is bidirectional and that microRNAs (miRNAs) in extracellular vesicles (EVs) secreted by human AECs regulate protein expression, antibiotic sensitivity, and biofilm formation by *P. aeruginosa*. Specifically, human EVs deliver miRNA let-7b-5p to *P. aeruginosa*, which systematically decreases the abundance of proteins essential for biofilm formation, including PpkA and ClpV1-3, and increases the ability of beta-lactam antibiotics to reduce biofilm formation by targeting the beta-lactamase AmpC. Let-7b-5p is bioinformatically predicted to target not only PpkA, ClpV1, and AmpC in *P. aeruginosa* but also the corresponding orthologs in *Burkholderia cenocepacia*, another notorious opportunistic lung pathogen, suggesting that the ability of let-7b-5p to reduce biofilm formation and increase beta-lactam sensitivity is not limited to *P. aeruginosa*. Here, we provide direct evidence for transfer of miRNAs in EVs secreted by eukaryotic cells to a prokaryote, resulting in subsequent phenotypic alterations in the prokaryote as a result of this interdomain communication. Since let-7–family miRNAs are in clinical trials to reduce inflammation and because chronic *P. aeruginosa* lung infections are associated with a hyperinflammatory state, treatment with let-7b-5p and a beta-lactam antibiotic in nanoparticles or EVs may benefit patients with antibiotic-resistant *P. aeruginosa* infections.**

host–pathogen communication | extracellular vesicles | exosomes | airway epithelial cells | RNAi

ESKAPE pathogens (*Enterococcus faecium*, *Staphylococcus aureus*, *Klebsiella pneumoniae*, *Acinetobacter baumannii*, *Pseudomonas aeruginosa*, and *Enterobacter* species) are the leading cause of nosocomial infections worldwide primarily due to their multidrug resistance (1). *P. aeruginosa* contributes to 5 to 10% of the acute exacerbations in chronic obstructive pulmonary disease (COPD), which afflicts 10% of the world's population and soon will be the third leading cause of death in the world (2–5). *P. aeruginosa* also chronically colonizes the lungs of ∼60% of adults with cystic fibrosis (CF), and its presence is strongly associated with reduced forced expiratory volume and a progressive loss of lung function (6–10). In addition, *P. aeruginosa* ventilator-associated pneumonia mortality rates can be as high as 30% (11). During chronic infection, *P. aeruginosa* establishes antibiotic-resistant biofilms, which are notoriously difficult to treat and are associated with serious adverse medical outcomes (12–14). Therefore, new strategies are needed to control recalcitrant chronic infections by *P. aeruginosa* and to prevent the formation of antibiotic-resistant biofilms.

Intercellular communication in the lungs is essential to maintain homeostasis and to raise an appropriate immune response to pathogens (15–18). In addition to cytokines and chemokines secreted by the myriad cell types in the lungs, eukaryotic cells also communicate by secreting extracellular vesicles (EVs) that contain proteins, lipid mediators, and microRNAs (miRNAs), which are 21- to 25-nucleotide–long noncoding RNAs that regulate gene expression (15, 16, 19, 20). EVs containing miRNAs have been identified in numerous biological samples including blood, urine, exhaled-breath condensates, and bronchoalveolar-lavage fluid (16, 18, 19, 21–23). When EVs fuse with target cells, they deliver their contents, including miRNAs that alter target-cell gene expression and function (24–28).

Cross-kingdom RNA interference (RNAi) mediated by EVs can play a crucial role in host–pathogen communication between plants and fungi (29–31). A few recent studies show that eukaryotic miRNAs affect prokaryotic organisms living in the gut: 1) Transfection of eukaryotic miRNAs into *Fusobacterium nucleatum* and *Escherichia coli* affects messenger RNA (mRNA) abundance and bacterial growth (32); 2) miR-30d given orally to mice increases the abundance of the commensal microbe *Akkermansia muciniphila* (33); and 3) Ginger-derived miRNAs are taken up by gut microbes, altering the microbiome (34). Although these studies

Significance

Pseudomonas aeruginosa **is one of the leading causes of hospital-acquired infections worldwide primarily due to its ability to develop antibiotic-resistant biofilms. This report describes a mechanism whereby human airway epithelial cells (AECs) increase the ability of antibiotics to kill *P. aeruginosa* and reduce the formation of drug-resistant biofilms. We demonstrate that human AECs secrete extracellular vesicles containing the microRNA let-7b-5p, that the vesicles deliver let-7b-5p to *P. aeruginosa*, and that let-7b-5p decreases biofilm formation and increases the ability of beta-lactam antibiotics to reduce biofilm formation by down-regulating key antibiotic-resistance and biofilm genes. A combination of let-7b, which is in clinical trials as an anti-inflammatory agent, and beta-lactam antibiotics may help combat antibiotic-resistant *P. aeruginosa* infections.**

Author contributions: K.K., Z.L., T.H.H., F.W.K., D.A.H., C.D.N., and B.A.S. designed research; K.K., A.N., R.B., L.B., Z.L., A.E.L., F.W.K., I.S.L., S.A.G., and S.K. performed research; S.K. and C.D.N. contributed new reagents/analytic tools; K.K. and T.H.H. analyzed data; and K.K., T.H.H., D.A.H., and B.A.S. wrote the paper.

The authors declare no competing interest.

This article is a PNAS Direct Submission.

[1]To whom correspondence may be addressed. Email: Katja.Koeppen@Dartmouth.edu.

This article contains supporting information online at https://www.pnas.org/lookup/suppl/doi:10.1073/pnas.2105370118/-/DCSupplemental.

Published July 6, 2021.

reveal that eukaryotic miRNAs affect bacteria, to our knowledge, there are no published studies demonstrating that eukaryotic EVs deliver miRNAs to bacteria or elucidating the mechanism of action of eukaryotic miRNAs in bacteria. Recently, we demonstrated that *P. aeruginosa* secretes outer-membrane vesicles that diffuse through mucus and fuse with human airway epithelial cells (AECs), delivering short interfering RNAs (siRNAs) that down-regulate the host immune response without direct contact between the bacterium and the host cells (35). Since siRNAs secreted by *P. aeruginosa* target eukaryotic genes, we hypothesized that eukaryotic miRNAs can also target bacterial genes to alter gene expression and phenotype. Motivated by the clinical challenge presented by antibiotic-resistant *P. aeruginosa* biofilms, we designed experiments to test whether EVs secreted by human AECs affect biofilm formation and also potentiate the ability of antibiotics to reduce these biofilms.

Results

EVs Reduce the Ability of *P. aeruginosa* to Form Biofilms. To assess whether EVs inhibit biofilm formation by *P. aeruginosa*, we conducted experiments using the crystal violet biofilm plate assay (36). We examined the effect of EVs at a concentration observed in bronchoalveolar-lavage fluid (18, 19) and found that EVs reduced biofilm formation by *P. aeruginosa* by 28% compared to vehicle control (Fig. 1*A*), while they did not significantly alter planktonic growth in biofilm plates (Fig. 1*D*).

EVs Enhance the Inhibition of Biofilm Formation by Antibiotics. We used the crystal violet biofilm plate assay (36) to determine whether EVs increase the ability of antibiotics to inhibit biofilm formation by *P. aeruginosa*. We observed that EVs and subinhibitory doses of the beta-lactam antibiotics aztreonam or carbenicillin significantly reduced biofilm formation (Fig. 1 *B* and *C*). The subinhibitory antibiotic concentration for biofilm formation by *P. aeruginosa* strain PA14 in the absence of EVs was 0.1 μg/mL for aztreonam and 5 μg/mL for carbenicillin. At these concentrations, antibiotics alone did not significantly alter biofilm formation by *P. aeruginosa* (*SI Appendix*, Fig. S1*A*). In combination with EVs, aztreonam decreased biofilm formation by 42% (Fig. 1*B*), while

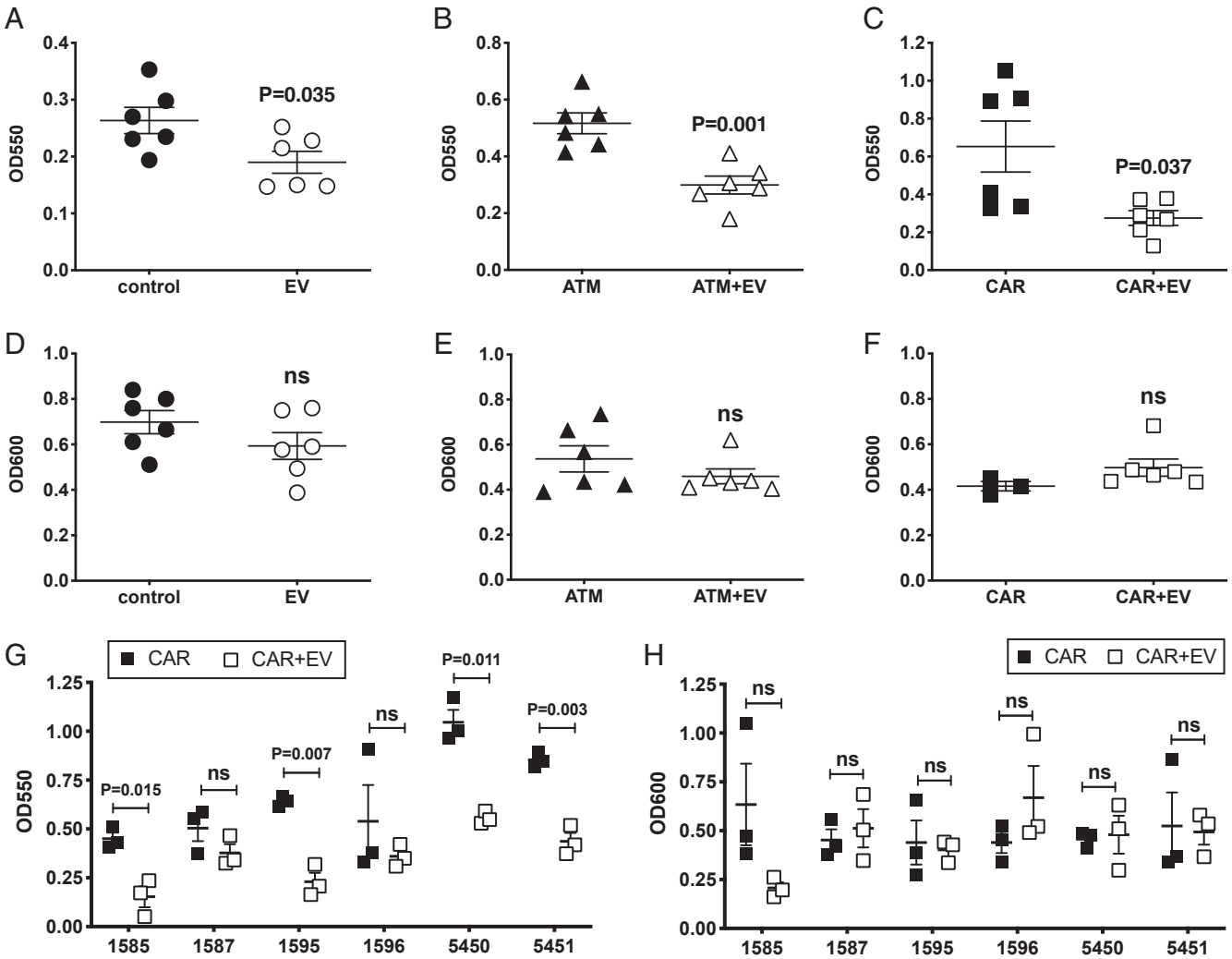

Fig. 1. EVs reduce biofilm formation by PA14 and increase the ability of beta-lactam antibiotics to reduce biofilm formation by PA14 and clinical isolates of *P. aeruginosa*. (*A–C*) EVs significantly inhibited biofilm formation by *P. aeruginosa* strain PA14 in the absence of antibiotics (*A*) as well as in the presence of 0.1 μg/mL aztreonam (ATM, *B*) and 5 μg/mL carbenicillin (CAR, *C*). (*D–F*) EVs did not significantly reduce planktonic growth of PA14 in the absence of antibiotics (*D*) or in the presence of subinhibitory concentrations of aztreonam (0.1 μg/mL, *E*) or carbenicillin (5 μg/mL, *F*). (*G*) EVs significantly reduced biofilm formation in the presence of 20 μg/mL carbenicillin in four of six clinical isolates of *P. aeruginosa*. (*H*) EVs did not significantly reduce planktonic growth of clinical isolates of *P. aeruginosa* in the presence of 20 μg/mL carbenicillin. Biofilms were measured after 24 h using the crystal violet 96-well plate biofilm assay (OD550) (36). Horizontal lines indicate means ± SEM. A two-tailed unpaired Welch's *t* test was used to calculate *P* values; $n = 3$ to 6 biological replicates with EVs isolated from three to six AEC donors; each data point is the average of three technical replicates; ns = not significant.

planktonic growth in biofilm plates was not significantly different (Fig. 1*E*). Likewise, EVs and carbenicillin together reduced biofilm formation by 58% (Fig. 1*C*) without significantly affecting planktonic growth (Fig. 1*F*). To determine whether these findings generalize to clinically relevant strains of *P. aeruginosa*, we assessed the ability of EVs to inhibit biofilm formation by six clinical isolates using a concentration of 20 μg/mL carbenicillin, which did not significantly reduce biofilm formation in the absence of EVs (*SI Appendix*, Fig. S1*B*). In combination, carbenicillin and EVs significantly decreased biofilm formation by four of the six clinical isolates we tested (Fig. 1*G*), demonstrating that the effect of EVs to prevent biofilm formation by *P. aeruginosa* is clinically relevant and not limited to the PA14 strain. EVs and carbenicillin together reduced biofilm formation by clinical isolate 1585 by 66%, 1595 by 64%, 5450 by 47%, and 5451 by 49% (Fig. 1*G*). EVs did not significantly decrease planktonic growth of *P. aeruginosa* in biofilm plates in the presence of carbenicillin in any of the six clinical isolates (Fig. 1*H*). We also assessed whether EVs increase the ability of aztreonam to inhibit biofilm formation by clinical isolates of *P. aeruginosa* and found that aztreonam and EVs together significantly decreased biofilm formation by clinical isolates 1585 and 1595 (*SI Appendix*, Fig. S2). EVs added to a subinhibitory concentration of aztreonam (0.5 μg/mL) decreased biofilm formation by clinical isolate 1585 by 65% (*SI Appendix*, Fig. S2*A*), concomitant with a 10-fold reduction in biofilm colony-forming units (CFUs) (*SI Appendix*, Fig. S2*B*), while planktonic growth (*SI Appendix*, Fig. S2*C*) and planktonic CFUs (*SI Appendix*, Fig. S2*D*) were not significantly altered compared to aztreonam alone. Likewise, 0.5 μg/mL aztreonam combined with EVs reduced biofilm formation by clinical isolate 1595 by 50% (*SI Appendix*, Fig. S2*E*) and decreased biofilm CFUs 10-fold (*SI Appendix*, Fig. S2*F*) but did not significantly affect planktonic growth (*SI Appendix*, Fig. S2*G*) or planktonic CFUs (*SI Appendix*, Fig. S2*H*). Finally, we assessed whether EVs could repress biofilm formation by the clinical isolate 1595 in the absence of antibiotics. While EVs did not significantly reduce biofilms as assessed by the crystal violet assay (*SI Appendix*, Fig. S2*I*), EVs alone significantly reduced the number of live bacteria in biofilms (*SI Appendix*, Fig. S2*J*) and reduced planktonic bacteria (*SI Appendix*, Fig. S2 *K* and *L*).

Studies were also conducted to examine the time course of EV inhibition of biofilm formation using the crystal violet plate assay. While no biofilms were detected after 6 h of incubation in any condition (*SI Appendix*, Fig. S3*A*), biofilms were detected after 12 h and increased further after 24 h for control as well as aztreonam and carbenicillin alone (*SI Appendix*, Fig. S3 *B* and *C*). EVs alone and in the presence of aztreonam or carbenicillin significantly decreased biofilm formation at 12 and 24 h compared to control, aztreonam alone, and carbenicillin alone (*SI Appendix*, Fig. S3 *B* and *C*).

EVs Increase the Beta-Lactam Sensitivity of Planktonic *P. aeruginosa*. To determine whether EVs also affect planktonic *P. aeruginosa*, we performed planktonic-growth assays over a range of 0 to 25 μg/mL aztreonam in the presence or absence of EVs. We found that EVs decreased both the minimal inhibitory concentration (MIC) and noninhibitory concentration (NIC) for aztreonam (Fig. 2). EVs reduced the MIC of aztreonam more than twofold in the presence of EVs (Fig. 2*A*). EVs also induced a sixfold decrease in the NIC of aztreonam (Fig. 2*B*). Moreover, in the presence of aztreonam (0.8 μg/mL, about one-half the MIC for *P. aeruginosa* strain PA14), EVs significantly reduced *P. aeruginosa* planktonic yield, (Fig. 2*C*) as well as CFUs (Fig. 2*D*), compared to *P. aeruginosa* not exposed to EVs. Aztreonam at a concentration close to one-half the MIC (0.8 μg/mL) significantly decreased planktonic growth compared to controls (Fig. 2*C*). There was a trend for EVs to reduce planktonic growth in the absence of aztreonam, but it did not reach statistical significance (Fig. 2*C*). Time-course data for the planktonic growth of *P. aeruginosa* in the presence or absence of EVs or 0.8 μg/mL

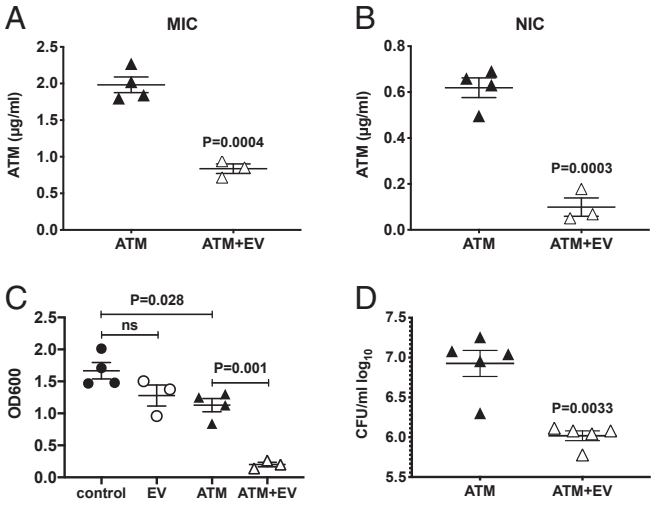

Fig. 2. EVs increase the beta-lactam sensitivity of planktonic *P. aeruginosa*. (*A*) EVs decreased the MIC of aztreonam (ATM) more than twofold (MIC = 2.0 μg/mL in control versus 0.8 μg/mL with EVs). (*B*) EVs decreased the NIC of aztreonam (NIC = 0.6 μg/mL in control versus 0.1 μg/mL with EVs). (*C* and *D*) In the presence of 0.8 μg/mL aztreonam (about one-half the MIC), EVs reduced planktonic growth of *P. aeruginosa* as determined by OD600 (*C*), as well as CFUs (*D*), after 24 h incubation. Horizontal lines indicate means ± SEM. A two-tailed unpaired Welch's *t* test was used to calculate *P* values; *n* = 3 to 5 biological replicates with EVs isolated from three to five AEC donors; each data point is the average of three technical replicates; ns = not significant.

aztreonam are shown in *SI Appendix*, Fig. S4*A*. Compared to aztreonam alone, aztreonam and EVs combined first led to a statistically significant reduction in planktonic growth at 15 h and 15 min and remained significantly repressed throughout the remainder of the time course (*SI Appendix*, Fig. S4*A*). Importantly, the finding that a combination of EVs and aztreonam decreases planktonic growth of *P. aeruginosa* was independent of the method used to isolate EVs (*SI Appendix*, Fig. S4*B*). Taken together with our biofilm experiments, these findings demonstrate that eukaryotic EVs increase the beta-lactam sensitivity of planktonic *P. aeruginosa* and reduce the ability of *P. aeruginosa* to form biofilms.

EVs Deliver Mature Human Let-7 miRNAs to *P. aeruginosa*. To begin to understand the mechanism whereby EVs reduce biofilm formation and increase beta-lactam antibiotic sensitivity, we performed an RNA sequencing (RNA-seq) analysis of EVs secreted by primary human AECs to test the hypothesis that EV RNAs target *P. aeruginosa* genes based on sequence complementarity, thus reducing the expression of proteins important for biofilm formation and beta-lactam antibiotic resistance. While EVs contain different kinds of molecules besides RNAs, including proteins, lipids, and metabolites, investigating the ability of EV RNAs to induce phenotypic changes in *P. aeruginosa* was the most tractable first step, because targeting predictions can be made based on miRNA–mRNA interactions. We identified several classes of small RNAs in EVs, including transfer RNA (tRNA), tRNA-like fragments, ribosomal RNA (rRNA), Piwi-interacting RNA (piRNA), long intergenic noncoding RNA (lincRNA), and miRNA, which is consistent with previous reports of RNA content of EVs secreted by other eukaryotic cells (25, 37–42). The five most abundant miRNAs in EVs secreted by AECs were miR-320a, let-7b-5p, let-7a-5p, miR-26a-5p, and miR-1246, accounting for >50% of all miRNA-sequence reads (*SI Appendix*, Table S1). To determine whether EVs can deliver miRNAs to *P. aeruginosa*, we conducted an RNA-seq analysis of *P. aeruginosa* exposed to EVs or vehicle. To avoid possible carryover

of EVs (and miRNA) attached to the outside of the bacteria, after exposure to EVs, the bacterial outer membrane was lysed with EDTA prior to RNA isolation. Cytoplasmic RNA was isolated after lysis of the cell wall and inner membrane. We detected six mature human miRNAs from the let-7 family (let-7a-5p, let-7b-5p, let-7c-5p, let-7e-5p, let-7f-5p, and let-7g-5p; *SI Appendix*, Fig. S5) in *P. aeruginosa* exposed to EVs, confirming our hypothesis that EVs can deliver miRNAs to the cytoplasm of *P. aeruginosa*. This is a direct demonstration that EVs secreted by a eukaryotic organism deliver miRNAs to a prokaryotic organism.

Let-7b-5p Is Predicted to Target Gene Expression in *P. aeruginosa*. We used the miRNA-targeting prediction algorithm IntaRNA (43) to assess whether the six miRNAs transferred to *P. aeruginosa* by EVs are predicted to regulate *P. aeruginosa* gene expression by targeting bacterial mRNAs. IntaRNA was designed to predict mRNA-target sites for eukaryotic miRNAs or bacterial small RNAs based on RNA–RNA interactions due to sequence similarity. For each potential miRNA and mRNA-target pair, IntaRNA calculates a combined energy score of the interaction that includes the free energy of hybridization as well as the free energy required for making the interaction sites accessible. The lower the energy score, the higher the likelihood of a successful targeting interaction. We found that, among the six miRNA that were transferred from EVs to *P. aeruginosa,* let-7b-5p had by far the most predicted high-quality *P. aeruginosa* gene targets (*SI Appendix*, Table S2). Because predicted let-7b-5p targets included genes that play an important role in biofilm formation, we selected let-7b-5p for follow-up experiments to test the hypothesis that let-7b-5p delivered by EVs reduces *P. aeruginosa* biofilm formation. To determine if the mechanism of action of *P. aeruginosa* targeting by let-7b-5p involves interaction of let-7b-5p with regulatory intergenic regions such as untranslated regions, rather than direct interaction within coding regions of genes, we used IntaRNA to predict let-7b-5p targeting of *P. aeruginosa* intergenic regions. We found that the average IntaRNA energy score for *P. aeruginosa* intergenic regions of −8.44 was significantly higher ($P = 0$), and thus much worse, than the average energy score for *P. aeruginosa* gene-coding regions of −14.62 (*SI Appendix*, Fig. S6). This suggests that let-7b-5p is more likely to regulate gene expression by directly targeting *P. aeruginosa* genes as opposed to intergenic regulatory regions.

Let-7b-5p Decreases *P. aeruginosa* Biofilm Formation. To provide direct evidence for the hypothesis that let-7b-5p reduces biofilm formation and increases the ability of beta-lactam antibiotics to reduce biofilm formation, we generated a PA14 strain (PA14-let7b) that expresses let-7b-5p under an arabinose-inducible promoter. We performed the crystal violet biofilm plate assay with PA14-let7b and a PA14 strain expressing the empty pMQ70 plasmid (PA14-vector). Biofilm formation by PA14-let7b was 90% less than biofilms formed by PA14-vector (Fig. 3*A*). This finding is consistent with the hypothesis that let-7b-5p decreases biofilm formation. By contrast, there was a small increase in planktonic PA14-let7b compared to PA14-vector (Fig. 3*B*). Recognizing that let-7b-5p concentrations in a genetically engineered strain might exceed those found in *P. aeruginosa* exposed to EVs, we conducted additional studies to examine whether a let-7b-5p antagomir inhibits the ability of EVs to reduce biofilm formation by *P. aeruginosa* growing on AECs.

An Let-7b-5p Antagomir Blocks the Ability of EVs to Reduce Biotic Biofilms. As we have shown previously (44–46), coculture of *P. aeruginosa* grown on a biotic surface, such as primary AECs, rather than an abiotic (nonliving) surface, like the 96-well plastic plates used in the crystal violet biofilm plate assay, represents a biologically relevant model to study the formation of *P. aeruginosa* biofilms that is comparable to in vivo models of *P. aeruginosa* infection (47). To test the hypothesis that let-7b-5p inhibits biotic

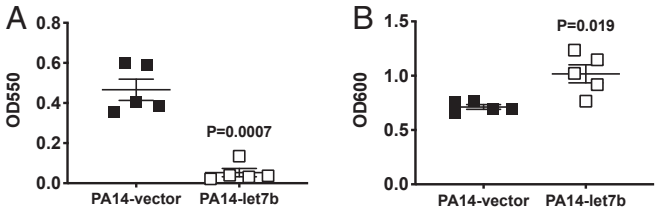

Fig. 3. Let-7b-5p reduces *P. aeruginosa* biofilm formation. (*A*) Biofilm formation by PA14-vector and PA14-let7b strains was measured in the presence of 100 mM arabinose and 300 μg/mL carbenicillin using the crystal violet 96-well plate biofilm assay (OD550) (36). Arabinose was used to induce let-7b-5p expression, and carbenicillin was used to inhibit growth of *P. aeruginosa* not containing the carbenicillin-resistant plasmid. (*B*) Let-7b-5p did not significantly reduce planktonic growth in biofilm plates (OD600) in the presence of 100 mM arabinose and 300 μg/mL carbenicillin and led to a significant increase in the planktonic fraction. Horizontal lines indicate means ± SEM. A two-tailed unpaired Welch's *t* test was used to calculate *P* values; $n = 5$ replicates of independent cultures of PA14-vector or PA14-let7b strains; each data point is the average of three technical replicates.

biofilm formation, *P. aeruginosa* was exposed to EVs isolated from AECs transfected with either a let-7b-5p antagomir (anti–let-7b EV) or a negative control antagomir (NC EV) as well as EVs isolated from untransfected AECs or phosphate-buffered saline (PBS) vehicle control. In crystal violet biofilm and planktonic-growth curve experiments (*SI Appendix*, Figs. S3 and S4*A*), we observed that it takes 12 h and more than 15 h, respectively, for EVs to reduce biofilm formation and planktonic growth of *P. aeruginosa*, presumably due to the long half-life of proteins targeted by let-7b-5p. We therefore preexposed planktonic *P. aeruginosa* to a biologically relevant concentration of EVs or PBS as a vehicle control for 18 h before adding the preexposed planktonic *P. aeruginosa* to the AECs. EVs used for preexposures were derived from the same airway-cell donor that was used in the subsequent coculture experiment, which was performed with a total of four donors. We imaged *P. aeruginosa* biofilms after 6 h of coculture, a time point that is too short for EVs produced by the AECs during coculture to affect biofilm formation, based on previous time-course experiments, but sufficient time to form biofilms on a biotic surface (46). Because *P. aeruginosa* is cytotoxic to AECs after 4 to 9 h (46), it was not possible to examine the effect of EVs directly secreted by AECs in coculture. Moreover, even if a prolonged coculture of *P. aeruginosa* and AECs were possible, such an experimental design would not allow for a no-EV control, as airway cells constitutively secrete EVs. The 18-h preexposures, as well as the 6-h cocultures, included a low concentration of aztreonam (0.1 μg/mL) that, by itself, did not affect planktonic growth or biofilm formation of *P. aeruginosa* (Fig. 1*E* and *SI Appendix*, Fig. S1*A*). *P. aeruginosa* exposed to PBS vehicle control formed robust biofilms after 6 h (Fig. 4*A*), while *P. aeruginosa* that had been preexposed to EVs for 18 h showed dramatically reduced biofilm formation (Fig. 4*B*). Likewise, preexposure of *P. aeruginosa* to EVs secreted by AECs that had been transfected with an NC EV induced a robust reduction of biofilm formation (Fig. 4*C*). By contrast, preexposure of *P. aeruginosa* to EVs harvested from AECs transfected with anti–let-7b EV did not significantly decrease *P. aeruginosa* biofilm formation (Fig. 4*D*). Representative overlay images of *P. aeruginosa* biofilms and AEC nuclei are provided in *SI Appendix*, Fig. S7 and demonstrate that coculture with *P. aeruginosa* did not disrupt the confluent monolayer of AECs, as shown previously by us (44–46). Initial attachment of PA14 to the apical surface of AECs after 1 h was similar in all experimental conditions (*SI Appendix*, Fig. S8), suggesting that EVs do not significantly inhibit the initial attachment step of *P. aeruginosa* biofilm formation. In summary, we demonstrate that the combination of EVs and a subinhibitory concentration of aztreonam (0.1 μg/mL) significantly reduces the

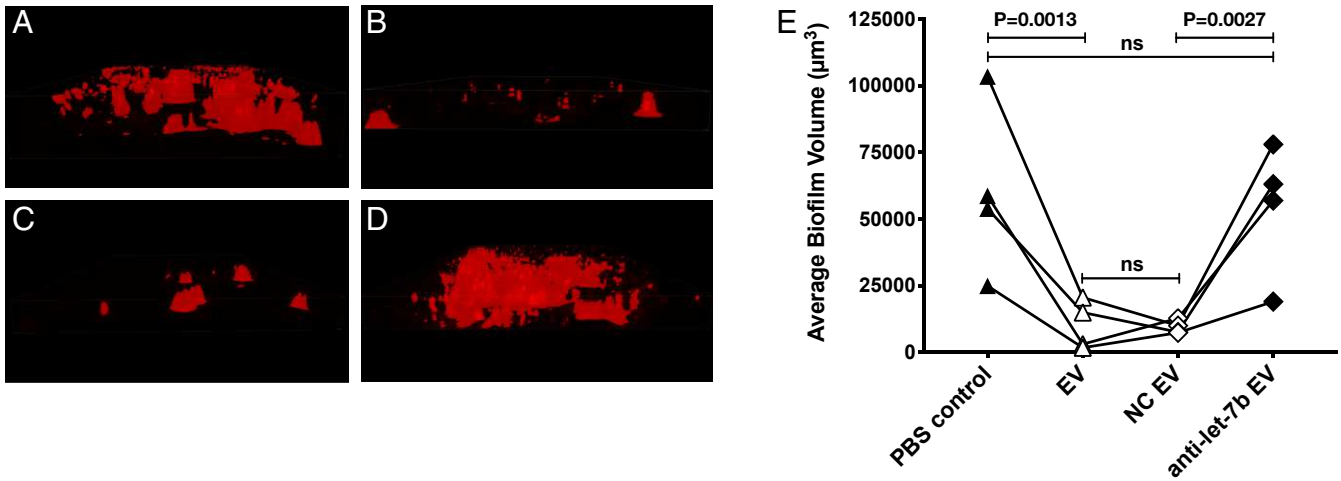

Fig. 4. EV-mediated reduction of biotic biofilm formation is reversed by a let-7b-5p antagomir. (*A*–*D*) Representative images of maximum intensity projections from z-stacks of biotic biofilms of *P. aeruginosa* PA14-mKO2 growing on AECs 6 h after inoculation. Since EV inhibition of planktonic growth required EV exposures >15 h to reduce target-protein abundance and because abiotic biofilms reached a maximal effect after 24 h, PA14-mKO2 was preexposed for 18 h to 0.1 μg/mL aztreonam plus either PBS vehicle control (*A*), EVs (*B*), EVs from AECs transfected with an NC EV (*C*), or EVs from AECs transfected with anti–let-7b EV (*D*), followed by a 6-h coculture with AECs for a total of 24 h. The 18-h preexposures, as well as the 6-h cocultures, included a low concentration of aztreonam (0.1 μg/mL) that, by itself, did not affect planktonic growth or biofilm formation of *P. aeruginosa*. (*E*) Summary of data. EVs (open triangles) reduced biofilm formation by 83% compared to *P. aeruginosa* exposed to PBS control (filled triangles). EVs containing the NC EV (open diamonds) also suppressed biofilm formation by 84% compared to *P. aeruginosa* exposed to PBS alone. By contrast, EVs containing anti–let-7b EV (filled diamonds) did not significantly decrease biofilm formation. Thus, let-7b-5p, in combination with aztreonam, dramatically reduces biofilm formation. Lines connect experiments conducted with AECs and EVs from the same donor in this paired experiment. Linear mixed-effects models with AEC donor as a random effect were used to calculate *P* values; $n = 4$ biological replicates with AECs and EVs from four donors; each data point is the average of five technical replicates (different areas of the same sample); ns = not significant.

formation of biofilms by *P. aeruginosa* on AECs and that this effect could be blocked with a let-7b-5p antagomir (Fig. 4*E*). Taken together, our studies demonstrate that let-7b-5p secreted in EVs inhibits biofilm formation by *P. aeruginosa*.

EVs Repress Aztreonam-Induced Proteins. To begin to explore the cellular mechanisms whereby EVs decrease the MIC and NIC for aztreonam and increase the ability of aztreonam to reduce biofilm formation, we conducted an unbiased proteomics analysis of *P. aeruginosa* exposed to vehicle or to EVs for 16 h in the presence or absence of 0.1 μg/mL aztreonam. Fold changes (FCs) and *P* values from the complete linear model as well as the group-wise comparisons for all 3,919 detected proteins are provided as Dataset S1. The beta-lactamase AmpC, which was a predicted let-7b-5p target with a good IntaRNA energy score in *P. aeruginosa*, was induced ($P < 0.05$) by aztreonam and repressed ($P < 0.05$) by the combination of EVs and aztreonam compared to aztreonam alone (Fig. 5). In addition, 15 proteins were induced by aztreonam by at least 50% ($P < 0.05$, and log2 fold change > 0.58). Eight of these aztreonam-induced proteins were significantly repressed in the presence of EVs and aztreonam compared to aztreonam alone (Fig. 5). Four additional aztreonam-induced proteins showed a tendency to be repressed in the presence of EVs, but this trend did not reach statistical significance. According to the comprehensive antibiotic resistance database (48), 8 of the 15 aztreonam-induced proteins have homology to beta-lactam–resistance proteins in other bacteria (*SI Appendix*, Table S3). Most notably, the hypothetical proteins PA14_48790 and PA14_16020, whose abundance was significantly increased by aztreonam and significantly decreased by the combination of EVs and aztreonam, are putative beta-lactamases based on protein-sequence homology. Five of the aztreonam-induced proteins (PopD, PopB, PbpG, PA14_50810, and PA14_48790) were significantly repressed by EVs in the presence and absence of aztreonam, suggesting that EVs counteract the natural response of *P. aeruginosa* to aztreonam (Fig. 5). These data indicate that EVs reduce the MIC and NIC of aztreonam by decreasing the abundance of several proteins that confer antibiotic resistance.

EVs Repress Proteins on the Biofilm-Formation Pathway. Kyoto Encyclopedia of Genes and Genomes (KEGG) (49) pathway activation analysis of the EV-induced FCs in protein abundance revealed biofilm formation as the only pathway predicted to be significantly down-regulated by EVs. This prediction is consistent with our observed phenotype of EV inhibition of biofilm formation. Seven proteins on the KEGG pathway "Biofilm Formation" (Hcp3, IcmF1, PpkA, ClpV2, ClpV3, TssK1 and HsiB1) were repressed ($P < 0.05$) by EVs compared to control samples in the absence of antibiotics, as well as EVs and aztreonam versus aztreonam alone (Fig. 6). Additional experiments, described in the next paragraph, demonstrate directly that let-7b-5p itself is sufficient to suppress proteins essential for biofilm formation.

Let-7b-5p Recapitulates EV-Mediated Reduction of *P. aeruginosa* Biofilm-Associated Proteins. To determine whether let-7b-5p is sufficient to suppress proteins that are essential for biofilm formation, we performed a second proteomics experiment comparing a *P. aeruginosa* strain expressing let-7b-5p (PA14-let7b) with an empty-vector control (PA14-vector) to assess the specific contribution of let-7b-5p to the observed EV-mediated repression of proteins on the biofilm-formation pathway. FCs, *P* values, and IntaRNA energy scores for all 4,218 detected proteins from the proteomics experiment with the let-7b-5p–expressing strain compared to the empty-vector strain of *P. aeruginosa* are provided as Dataset S2. Looking at the correlation between let-7b-5p–mediated protein-level changes and IntaRNA target predictions for let-7b-5p in *P. aeruginosa*, there was a weak but statistically significant ($P = 0.02$) positive correlation between proteins with an IntaRNA energy score in the top 10% and protein-level log2 FCs with let-7b-5p compared to the empty-vector control. By contrast, there was no significant correlation between proteins in the bottom 10% of energy scores and log2 FC. KEGG pathway-activation analysis of

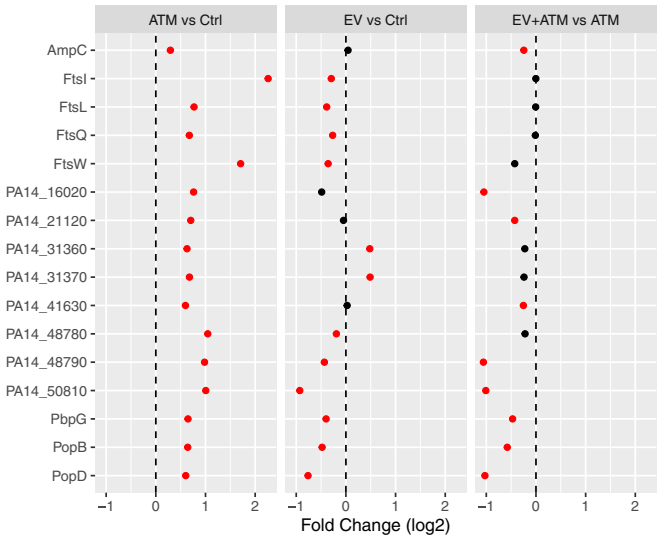

Fig. 5. EVs repress aztreonam-induced proteins. A total of 16 *P. aeruginosa* proteins (listed on the *y*-axis) were significantly induced by 0.1 μg/mL aztreonam (ATM) compared to controls (Ctrl, *Left*). Log2 FCs for the comparisons are shown on the *x*-axis. Proteins with $P < 0.05$ are depicted as filled red circles, while proteins with $P > 0.05$ are shown as filled black circles. Compared to controls, EVs significantly repressed 10 of the aztreonam-induced proteins (*Middle*). When comparing protein levels of *P. aeruginosa* exposed to EVs plus aztreonam to *P. aeruginosa* exposed to aztreonam only *(Right)*, all but three aztreonam-induced proteins showed lower abundance in the presence of EVs, with nine proteins showing significant repression ($P < 0.05$). Linear models in R were used to calculate *P* values; $n = 4$ biological replicates with EVs isolated from four AEC donors.

the let-7b-5p–induced FCs in protein abundance confirmed that the biofilm-formation pathway was repressed by let-7b-5p ($P = 0.0005$), corroborating our previous observation that EVs systematically inhibit the biofilm-formation pathway. Of 29 proteins whose abundance was altered ($P < 0.05$) by the presence of let-7b-5p, 24 were down-regulated (Fig. 6). Of the 15 proteins with the largest negative FCs in response to let-7b-5p, 7 (Hcp3, IcmF1, PpkA, ClpV2, ClpV3, TssK1 and HsiB1) were also significantly repressed by EVs in the presence and absence of antibiotics, and 5 showed a trend of reduced protein levels in response to EVs that did not reach statistical significance (Fig. 6). A table of all 48 proteins that were decreased ($P < 0.05$ and log2 FC < -0.58) in the let-7b-5p–expressing strain compared to the empty-vector control is provided in *SI Appendix*, Table S4. This list of proteins whose abundance was reduced by let-7b-5p is not only enriched for proteins on the biofilm-formation pathway but also contains many proteins associated with the bacterial secretion system, the two-component system, and bacterial chemotaxis (*SI Appendix*, Table S4). In summary, these experiments demonstrate that let-7b-5p reduces the abundance of proteins that are essential for biofilm formation by *P. aeruginosa*.

Discussion

Here, we discovered that a miRNA, let-7b-5p, in EVs secreted from a eukaryotic host, is delivered to and regulates the protein abundance of biofilm genes in a prokaryotic organism and that this interdomain RNAi results in phenotypic alterations in the prokaryote, including increased sensitivity to antibiotics and reduced biofilm formation. We found that let-7b-5p–containing EVs secreted by AECs reduced biofilm formation by *P. aeruginosa* and increased sensitivity to the beta-lactam antibiotic aztreonam and that the combination of EVs with beta-lactam antibiotics potentiated the ability of EVs to reduce biofilm formation by *P. aeruginosa* strain PA14 as well as clinical isolates. Moreover, let-7b-5p itself significantly suppressed biofilm formation by *P. aeruginosa*, and an let-7b-5p antagomir inhibited the ability of EVs to reduce biofilm formation.

Proteomics experiments revealed that EVs systematically repress aztreonam-induced proteins and proteins on the biofilm-formation pathway. EVs, as well as let-7b-5p, systematically inhibited proteins on the biofilm-formation pathway, including ClpV2, ClpV3, Hcp3, HsiB1, IcmF1, PpkA and Tssk1 (Fig. 6). It has been previously shown that a clpV2 knockout strain of *Enterobacter cloacae* exhibited a significant decrease in biofilm formation (50), that a clpV3 deletion resulted in smaller *P. aeruginosa* biofilms (51), and that a ppkA deletion mutant of *P. aeruginosa* has a biofilm-formation defect (52). In addition, the expression of the hemolysin-coregulated protein Hcp3, an important effector protein of the type-VI secretion system, is increased in biofilm-forming compared to non-biofilm-forming clinical isolates of *P. aeruginosa* and is associated with more severe symptoms such as longer hospitalization (53). Collectively, our findings explain how the combination of beta-lactam antibiotics and EVs reduce planktonic growth and biofilm formation of *P. aeruginosa* more robustly than either of these factors alone.

To assess whether let-7b-5p regulation may be limited to *P. aeruginosa* or whether it generalizes to other common opportunistic lung pathogens, we used IntaRNA to predict let-7b-5p targets in *Burkholderia cenocepacia*, *Streptococcus pneumoniae*, and *Staphylococcus aureus*. Even though the mean IntaRNA energy score for *P. aeruginosa* genes of −14.62 was significantly lower (better) than those of *B. cenocepacia* (−13.44), *S. pneumoniae* (−12.19), or *S. aureus* (−11.32) (*SI Appendix*, Fig. S6), there was significant overlap between predicted gene targets that were in the top 10% of energy scores for both *P. aeruginosa* and *B. cenocepacia* ($P = 0.0007$) as well as *P. aeruginosa* and *S. pneumoniae* ($P = 0.008$) but not *P. aeruginosa* and *S. aureus* ($P = 0.28$). Among the genes that were in the top 10% by energy score for both *P. aeruginosa* and *B. cenocepacia* are the beta-lactamase AmpC and the serine/threonine protein kinase ppkA, which has been previously described to be essential for biofilm formation (52). Additional experiments beyond the scope of this study are needed to elucidate the extent to which EVs and let-7b-5p inhibit biofilm formation and increase antibiotic sensitivity of other lung pathogens and how these phenotypic changes of the pathogen affect the host.

A very recent study found that RSV infection increased the secretion of EVs by an AEC line and that the EVs promoted biofilm formation by *P. aeruginosa* compared to EVs secreted by uninfected cells (54). The study reported that respiratory syncytial virus (RSV) increased the secretion of EVs containing a transferrin–iron complex on the extravesicular surface that promoted biofilm growth. Thus, taken together with our study, this report reveals that EVs secreted by AECs can regulate biofilm formation, both in a positive and negative way, by multiple mechanisms. Another recently published paper demonstrated that EVs secreted by human mesenchymal stromal cells reduced the load of *P. aeruginosa* as well as proinflammatory cytokines and neutrophils in murine bronchoalveolar lavage fluid (BALF) and that the effect was mediated by miRNA-466, although the mechanism of action was not elucidated (55). Thus, taken together with our data, there is evidence that miRNA-466 and let-7b-5p reduce *P. aeruginosa* infection.

One limitation of our study is that proteomics experiments were not able to measure about one-third of *P. aeruginosa* proteins, which impairs our ability to perfectly correlate IntaRNA targeting predictions with observed protein-level changes. For example, the top 10% of predicted let-7b-5p targets included 10 transcription factors that were not detected at the protein level in proteomics experiments, presumably due to their low abundance. A let-7b-5b–mediated reduction in the protein levels of these transcription factors would be predicted to affect a host of other downstream genes and proteins that are not direct targets of let-7b-5p but whose expression is regulated by these transcription factors. Such

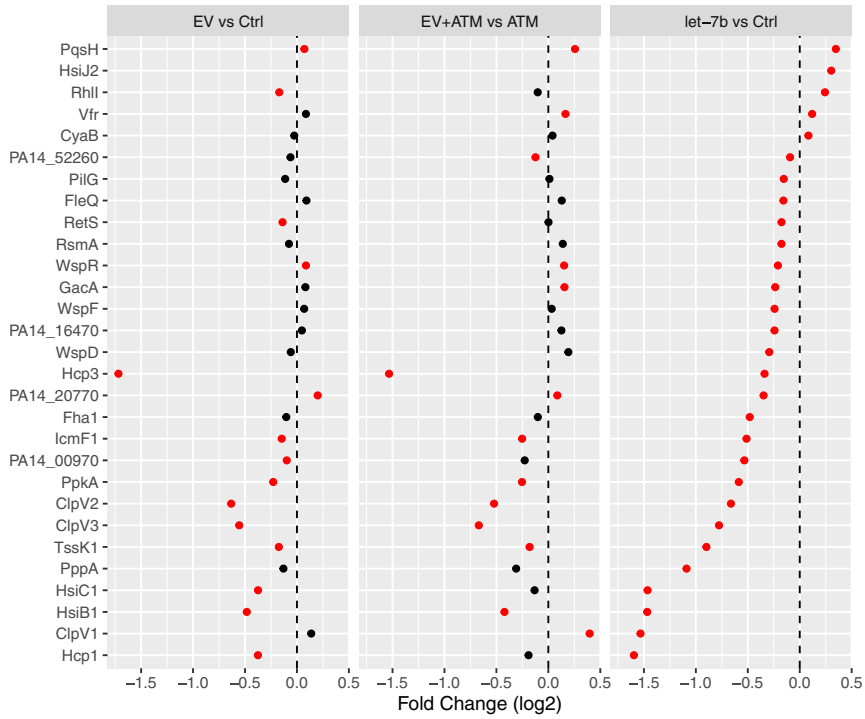

Fig. 6. Let-7b-5p and EVs systematically repress proteins associated with biofilm formation. A total of 29 proteins from the KEGG pathway "Biofilm Formation" that were differentially expressed in the presence of let-7b-5p compared to the empty-vector control (*Right*) are listed on the *y*-axis. Protein-level changes with EV plus aztreonam (ATM) compared to aztreonam alone (*Middle*) and EV compared to controls in the absence of antibiotics (*Left*) are shown for comparison. Log2 FCs for the different comparisons are shown on the *x*-axis. Proteins with $P < 0.05$ are depicted as filled red circles, while proteins with $P > 0.05$ are shown as filled black circles. Compared to the empty-vector control, let-7b-5p expression significantly decreased the abundance of 24 out of 29 proteins on the biofilm-formation pathway (*Right*). Seven of these let-7b-5p–repressed proteins (Hcp3, IcmF1, PpkA, ClpV2, ClpV3, Tssk1, and HsiB1) were also significantly reduced by EVs in the presence and absence of aztreonam. Linear models in R were used to calculate *P* values; $n = 4$ biological replicates with EVs isolated from four AEC donors (*Left* and *Middle*) or $n = 3$ replicates of independent cultures of the empty-vector or let-7b-5p–expressing strains grown in the presence of 150 μg/mL carbenicillin to select for *P. aeruginosa* containing the let-7b-5p expression plasmid.

indirect effects of let-7b-5p targeting may help explain why IntaRNA energy scores and let-7b-5p proteomics data do not correlate more strongly and why some proteins that are not predicted to be direct targets of let-7b-5p nevertheless have large reductions in protein abundance in response to let-7b-5p. Moreover, our study focuses on let-7b-5p and does not investigate the effect of other EV contents on *P. aeruginosa* protein abundance, biofilm formation, or antibiotic sensitivity. We chose let-7b-5p because it is one of the most abundant miRNAs in EVs, is transferred to *P. aeruginosa* following EV exposure, and has a large number of predicted targets in *P. aeruginosa*. While we cannot exclude the possibility that other EV contents contribute to the phenotypic changes in *P. aeruginosa*, the fact that the let-7b-5p antagomir completely blocks the ability of EVs to reduce biofilm formation suggests that let-7b-5p is sufficient to achieve the full effect. Another limitation of the present study is that the combination of EVs and aztreonam used did not completely eliminate either planktonic *P. aeruginosa* or biofilm formation, raising the issue of clinical and therapeutic utility of EVs to treat antibiotic-resistant clinical stains of *P. aeruginosa*. In experiments in progress that are beyond the scope of the present study, we are examining the dose-dependent effects of EVs and aztreonam on antibiotic-resistant clinical strains *of P. aeruginosa* in vitro and in a mouse model of infection.

Many eukaryotic miRNAs secreted in EVs, including let-7b, play an important role in several respiratory diseases including COPD, idiopathic pulmonary fibrosis, and asthma—all diseases that cause significant morbidity and mortality (15, 16, 20, 56, 57). For example, let-7b-5p is down-regulated in EVs isolated from the bronchoalveolar-lavage fluid of patients with influenza-induced acute respiratory distress syndrome (18) and is reduced in bronchial brushings isolated from CF patients versus non-CF donors (58). Moreover, let-7b-5p is anti-inflammatory and suppresses the innate immune response of the host to pathogens (21–23). As of 2020, there were six clinical trials using members of the let-7 family to treat a variety of diseases including obesity, diabetes, and cancer (21, 59) but none to treat bacterial infections. Because chronic, antibiotic-resistant *P. aeruginosa* lung infections are associated with a hyperinflammatory state, treatment with let-7b-5p in combination with beta-lactam antibiotics may benefit patients with chronic *P. aeruginosa* lung infections in two ways: 1) by increasing the antibiotic sensitivity of planktonic *P. aeruginosa* and inhibiting the formation of antibiotic-resistant biofilms and 2) by acting on host cells in the lungs to counteract the hyperinflammatory milieu, which is a major driver of lung damage (12–14, 60–65). Future studies are focused on developing an approach utilizing let-7b-5p in combination with beta-lactam antibiotics to combat antibiotic-resistant, recalcitrant *P. aeruginosa* lung infections of this ESKAPE pathogen that causes considerable morbidity and mortality worldwide.

Materials and Methods

Bacterial Strains and Culture. *P. aeruginosa* strain PA14, as well as six CF clinical isolates of *P. aeruginosa* (66), was grown in Luria broth (LB, Thermo Fisher Scientific), which was used in all *P. aeruginosa* assays. The clinical isolates, which were originally isolated from sputum samples of six independent CF patients, included three mucoid and three nonmucoid strains and have been previously characterized (67). A PA14 strain that expresses let-7b-5p under the control of an arabinose-inducible promoter and an empty-vector control strain were produced by transforming PA14 with a pMQ70 expression vector (68) containing either the mature let-7b-5p sequence as an insert (PA14-let7b) or

no insert (PA14-vector). Both strains were cultured in the presence of 100 mM arabinose (Sigma-Aldrich, catalog no. A3256) and 300 μg/mL carbenicillin (Sigma-Aldrich, catalog no. C1389). Expression of let-7b-5p in PA14-let7b was verified by RT-qPCR using a TaqMan gene-expression assay for hsa-let-7b-5p (Thermo Fisher Scientific, catalog no. 4427975, assay ID 002619). During exposure of *P. aeruginosa* to EVs, the beta-lactam antibiotics aztreonam (MP Biomedicals, catalog no. 150415) or carbenicillin (Sigma-Aldrich, catalog no. C1389-5G) were added to the culture medium at the indicated concentrations.

Culture of Human AECs and EV Isolation. De-identified primary human AECs from six donors were obtained from Scott Randell (University of North Carolina at Chapel Hill, Chapel Hill, NC) and cultured as previously described (69, 70). Briefly, cells were grown in BronchiaLife basal medium (Lifeline Cell Technology, catalog no. LM-0007) supplemented with the BronchiaLife B/T LifeFactors Kit (Lifeline Cell Technology, catalog no. LS-1047) as well as 10,000 U/mL penicillin and 10,000 μg/mL streptomycin (Sigma-Aldrich, catalog no. P4333). EVs were purified from AEC culture supernatants (passages 4 to 8; results were independent of passage number) using the ExoQuick-TC EV isolation kit (System Biosciences, catalog no. EXOTC50A-1) or OptiPrep (Sigma-Aldrich) gradient ultracentrifugation. Details on EV isolation, quantification, and characterization are described in *SI Appendix*. When exposing *P. aeruginosa* to EVs, we used a ratio of 500 or 1,000 EVs per bacterium and a concentration of 5×10^9 EV/mL, corresponding to a concentration of EVs measured in AEC culture supernatants by us, as well as in human bronchoalveolar-lavage fluid (18, 19).

Planktonic-Growth Curves and MIC and NIC Calculation. The MIC and NIC of aztreonam were determined as described by us and others (71, 72). Briefly, 5,000 CFUs of *P. aeruginosa* were incubated with or without 5×10^9 EVs/mL in 200 μl LB, with eight different concentrations of aztreonam (0 to 25 μg/mL) in triplicate for 24 h in a plate reader at 37 °C. The optical density at 600 nm (OD600) was recorded every 15 min, and the MIC and NIC for aztreonam were calculated by fitting the growth-curve data with a Gompertz function (71, 72). CFU/mL for viable planktonic bacteria were obtained by dilution plating of supernatants.

Crystal Violet Biofilm Assay. We assessed the effect of EVs on biofilm formation by *P. aeruginosa* using the crystal violet 96-well plate biofilm assay as described (36). PA14 or clinical isolates of *P. aeruginosa* were plated at 1×10^6 bacteria per 100 μl LB and grown for 24 h in the presence of 5×10^9/mL EVs or phosphate-buffered saline (PBS) vehicle control and subthreshold concentrations of antibiotics, defined as concentrations that by themselves did not significantly reduce biofilm formation. Antibiotic concentrations that did not inhibit biofilm formation in the absence of EVs were 0.1 μg/mL aztreonam for PA14 and 0.5 μg/mL aztreonam for CF clinical isolates of *P. aeruginosa* as well as 5 μg/mL carbenicillin for PA14 and 20 μg/mL carbenicillin for CF clinical isolates. For time-course experiments, *P. aeruginosa* strain PA14 was plated at 1×10^6 bacteria per 100 μl LB and grown for 6, 12, or 24 h in the presence or absence of 5×10^9/mL EVs and in the presence or absence of 0.1 μg/mL aztreonam or 5 μg/mL carbenicillin. Viable bacteria in biofilm fractions were quantified by dilution plating and calculation of CFU/mL as described previously (73).

RNA-seq of EVs. The sequencing of EV small RNA content was performed by System Biosciences. Briefly, EVs were harvested from 15 mL cell-culture supernatants using the ExoQuick-TC EV isolation kit. Total EV RNA was isolated with the SeraMir Exosome RNA Purification Column kit (System Biosciences, catalog no. RA808A-1), and small RNA libraries were constructed with the CleanTag Small RNA Library Preparation Kit (TriLink Biotechnologies, catalog no. L-3206). Size-selected libraries were sequenced as 75-nucleotide single-end reads on Illumina Next Seq. For additional details, refer to *SI Appendix*.

Transfer of miRNA to *P. aeruginosa*: RNA-seq of *P. aeruginosa*. *P. aeruginosa* (1.5×10^7 CFU) were exposed to PBS vehicle control or EVs (5×10^9 EV/mL) for 6 h. To avoid possible carryover of EVs (and miRNA) attached to the outside of the bacteria, the bacteria were washed with PBS, and the bacterial outer membrane was lysed with EDTA to release periplasmic contents and factors associated with the bacterial outer membrane and periplasm (74–76). The cells were then washed again in PBS, and cytoplasmic RNA was harvested after lysis of the bacterial cell wall and inner membrane. Total RNA was isolated with the miRNeasy Mini Kit (Qiagen, catalog no. 217004), including the on-column DNA digestion. Sequencing libraries were prepared with the QIAseq small RNA kit (Qiagen), and 75-bp single-end reads were generated using an Illumina MiniSeq. Sequences that did not map to the PA14 reference genome were aligned to the human genome using CLC Genomics Workbench software (Qiagen).

IntaRNA Target Prediction. The IntaRNA miRNA target prediction algorithm (43) was used to assess whether human miRNAs transferred to *P. aeruginosa* by EVs might regulate *P. aeruginosa* gene expression by targeting bacterial mRNAs. IntaRNA predictions using *Pseudomonas aeruginosa* UCBPP-PA14 reference sequences and standard parameters were run to obtain energy scores as a measure of the likelihood of RNA–RNA interaction based on sequence similarity. The IntaRNA energy score comprises the free energy of hybridization as well as the free energy required for making the interaction sites accessible. In addition, IntaRNA target predictions of let-7b-5p in *P. aeruginosa* intergenic regions and of other common lung pathogens were made using standard parameters and reference sequences for the following bacterial strains: *B. cenocepacia* J2315, a multidrug-resistant CF clinical isolate; *S. pneumoniae* R6, the derivative of a clinical isolate; and *S. aureus* COL, a methicillin-resistant clinical isolate. Fisher's exact test was used to calculate *P* values for the overlap of targets in the top 10% of energy scores between *P. aeruginosa* and each of the other three species of bacteria.

Transfection of AECs with a Let-7b-5p Antagomir. To demonstrate that the ability of EVs to decrease biofilm formation in the presence of beta-lactam antibiotics is mediated by let-7b-5p, AECs were transfected with 10 nM mirVana miRNA Inhibitor for hsa-let-7b-5p (Thermo Fisher Scientific, catalog no. 4464084) or 10 nM mirVana miRNA Inhibitor Negative Control no. 1 (Thermo Fisher Scientific, catalog no. 4464076) using Lipofectamine RNAiMAX Transfection Reagent (Thermo Fisher Scientific, catalog no. 13778150). A total of 24 h after transfection, EVs were isolated from cell-culture supernatants and quantified as described in *Supplementary Materials and Methods* in *SI Appendix*.

Biotic Biofilm Assay. The effect of EVs on the formation of *P. aeruginosa* on a biotic surface was determined by methods developed and described in detail previously by us (45, 46). Briefly, primary human AECs from four donors were grown as confluent monolayers on glass coverslips, and 3×10^6 orange fluorescent PA14 that had been preexposed to EVs from the respective AEC donors (or PBS control) in the presence of 0.1 μg/mL aztreonam were added to the apical side of the AEC monolayers and imaged over a 6-h period. A full description of the experiment can be found in *SI Appendix*.

Proteomic Analysis of *P. aeruginosa*. *P. aeruginosa* strain PA14 (1×10^7 CFU) was exposed to EVs (1×10^{10}) secreted by AECs ($n = 3$) or vehicle controls in the presence or absence of 0.1 μg/mL aztreonam and incubated for 16 h at 37 °C and 225 rpm. In a second set of experiments, the let-7b-5p–expressing strain PA14-let7b and the empty-vector control PA14-vector were grown in triplicate with 150 μg/mL carbenicillin for 16 h at 37 °C and 225 rpm. Arabinose was not included in this experiment because the levels of let-7b-5p that are produced by the leaky promotor without arabinose induction are closer to the amount of let-7b-5p delivered to *P. aeruginosa* by EVs and thus more biologically relevant. Refer to *SI Appendix* for details on sample processing and mass spectrometry. Samples were run in two batches of eight samples (two from each group). To account for batch effects, log2 transformed peak intensities were analyzed using linear models in R (77) by including batch as a factor in the model. Figures were generated using the ggplot2 package (78). Systematic KEGG-pathway activation analysis was performed with the help of the KEGGREST package in R (79) as previously described (80, 81). Briefly, under the null hypothesis, about half of the proteins associated with any KEGG pathway would be expected to respond to EV exposure with an FC > 0, while the other half would respond with an FC < 0. Statistically significant divergence from this 50% split was assessed using binomial tests based on the FCs of all proteins associated with a KEGG pathway.

Statistical Analysis. Data were analyzed with Prism 8 for macOS (version 8.4.3, Graphpad) and the R software environment for statistical computing and graphics (77) (version 4.0.2) using appropriate statistical methods as indicated in the figure legends. The R package nlme (version 3.1-152) was used to calculate *P* values from linear mixed-effect models (82).

Data Availability. RNA-seq data have been deposited in the National Center for Biotechnology Information Gene Expression Omnibus under accession nos. GSE174690 and GSE174710. All other study data are included in the article and/or supporting information.

ACKNOWLEDGMENTS. This work was supported by CF Foundation Grants STANTO19G0, STANTO20P0, STANTO19R0, and HOGAN19G0; NIH Grants P30-DK117469, R01HL151385, P20-GM113132, and 2R01AI081838; NSF Grants MCB 1817342 and IOS 2017879; Human Frontier Science Program Grant RGY0077/2020; Norris Cotton Cancer Center Core Grant 5P30CA023108; and a Dartmouth Burke Award.

1. M. S. Mulani, E. E. Kamble, S. N. Kumkar, M. S. Tawre, K. R. Pardesi, Emerging strategies to combat ESKAPE pathogens in the era of antimicrobial resistance: A review. *Front. Microbiol.* **10**, 539 (2019).
2. S. A. Novosad, A. F. Barker, Chronic obstructive pulmonary disease and bronchiectasis. *Curr. Opin. Pulm. Med.* **19**, 133–139 (2013).
3. D. Lieberman, D. Lieberman, Pseudomonal infections in patients with COPD: Epidemiology and management. *Am. J. Respir. Med.* **2**, 459–468 (2003).
4. S. Sethi, Infection as a comorbidity of COPD. *Eur. Respir. J.* **35**, 1209–1215 (2010).
5. A. Fazleen, T. Wilkinson, Early COPD: Current evidence for diagnosis and management. *Ther. Adv. Respir. Dis.* **14**, 1753466620942128 (2020).
6. B. A. Stanton, Effects of *Pseudomonas aeruginosa* on CFTR chloride secretion and the host immune response. *Am. J. Physiol. Cell Physiol.* **312**, C357–C366 (2017).
7. J. C. Davies, I. Martin, New anti-pseudomonal agents for cystic fibrosis- still needed in the era of small molecule CFTR modulators? *Expert Opin. Pharmacother.* **19**, 1327–1336 (2018).
8. J. E. Pittman, G. Cutting, S. D. Davis, T. Ferkol, R. Boucher, Cystic fibrosis: NHLBI workshop on the primary prevention of chronic lung diseases. *Ann. Am. Thorac. Soc.* **11** (suppl. 3), S161–S168 (2014).
9. J. F. Collawn, S. Matalon, CFTR and lung homeostasis. *Am. J. Physiol. Lung Cell. Mol. Physiol.* **307**, L917–L923 (2014).
10. T. S. Cohen, A. Prince, Cystic fibrosis: A mucosal immunodeficiency syndrome. *Nat. Med.* **18**, 509–519 (2012).
11. B. J. Williams, J. Dehnbostel, T. S. Blackwell, *Pseudomonas aeruginosa*: Host defence in lung diseases. *Respirology* **15**, 1037–1056 (2010).
12. J. Dreier, P. Ruggerone, Interaction of antibacterial compounds with RND efflux pumps in *Pseudomonas aeruginosa*. *Front. Microbiol.* **6**, 660 (2015).
13. M. Puzari, P. Chetia, RND efflux pump mediated antibiotic resistance in Gram-negative bacteria *Escherichia coli* and *Pseudomonas aeruginosa*: A major issue worldwide. *World J. Microbiol. Biotechnol.* **33**, 24 (2017).
14. W. C. Rutter, D. R. Burgess, D. S. Burgess, Increasing incidence of multidrug resistance among cystic fibrosis respiratory bacterial isolates. *Microb. Drug Resist.* **23**, 51–55 (2017).
15. B. Sastre, J. A. Cañas, J. M. Rodrigo-Muñoz, V. Del Pozo, Novel modulators of asthma and allergy: Exosomes and microRNAs. *Front. Immunol.* **8**, 826 (2017).
16. J. Chen, C. Hu, P. Pan, Extracellular vesicle microRNA transfer in lung diseases. *Front. Physiol.* **8**, 1028 (2017).
17. V. Neudecker *et al*., Neutrophil transfer of *miR-223* to lung epithelial cells dampens acute lung injury in mice. *Sci. Transl. Med.* **9**, eaah5360 (2017).
18. N. Scheller *et al*., Proviral microRNAs detected in extracellular vesicles from bronchoalveolar lavage fluid of patients with influenza virus-induced acute respiratory distress syndrome. *J. Infect. Dis.* **219**, 540–543 (2019).
19. D. A. Armstrong *et al*., Pulmonary microRNA profiling: Implications in upper lobe predominant lung disease. *Clin. Epigenetics* **9**, 56 (2017).
20. T. S. Cohen, Role of microRNA in the lung's innate immune response. *J. Innate Immun.* **9**, 243–249 (2017).
21. M. E. Gilles, F. J. Slack, Let-7 microRNA as a potential therapeutic target with implications for immunotherapy. *Expert Opin. Ther. Targets* **22**, 929–939 (2018).
22. L. N. Schulte, A. Eulalio, H. J. Mollenkopf, R. Reinhardt, J. Vogel, Analysis of the host microRNA response to Salmonella uncovers the control of major cytokines by the let-7 family. *EMBO J.* **30**, 1977–1989 (2011).
23. G. G. Teng *et al*., Let-7b is involved in the inflammation and immune responses associated with *Helicobacter pylori* infection by targeting Toll-like receptor 4. *PLoS One* **8**, e56709 (2013).
24. J. Lötvall *et al*., Minimal experimental requirements for definition of extracellular vesicles and their functions: A position statement from the International Society for Extracellular Vesicles. *J. Extracell. Vesicles* **3**, 26913 (2014).
25. J. W. Choi, J. H. Um, J. H. Cho, H. J. Lee, Tiny RNAs and their voyage via extracellular vesicles: Secretion of bacterial small RNA and eukaryotic microRNA. *Exp. Biol. Med. (Maywood)* **242**, 1475–1481 (2017).
26. F. A. Lefebvre, E. Lécuyer, Small luggage for a long journey: Transfer of vesicle-enclosed small RNA in interspecies communication. *Front. Microbiol.* **8**, 377 (2017).
27. L. B. Jones *et al*., Pathogens and their effect on exosome biogenesis and composition. *Biomedicines* **6**, 79 (2018).
28. R. Gupta *et al*., Intercellular communication between airway epithelial cells is mediated by exosome-like vesicles. *Am. J. Respir. Cell Mol. Biol.* **60**, 209–220 (2019).
29. M. Wang, R. A. Dean, Movement of small RNAs in and between plants and fungi. *Mol. Plant Pathol.* **21**, 589–601 (2020).
30. E. Woith, G. Fuhrmann, M. F. Melzig, Extracellular vesicles-connecting kingdoms. *Int. J. Mol. Sci.* **20**, 5695 (2019).
31. Q. Cai *et al*., Plants send small RNAs in extracellular vesicles to fungal pathogen to silence virulence genes. *Science* **360**, 1126–1129 (2018).
32. S. Liu *et al*., The host shapes the gut microbiota via fecal microRNA. *Cell Host Microbe* **19**, 32–43 (2016).
33. S. Liu *et al*., Oral administration of miR-30d from feces of MS patients suppresses MS-like symptoms in mice by expanding *Akkermansia muciniphila*. *Cell Host Microbe* **26**, 779–794.e8 (2019).
34. Y. Teng *et al*., Plant-derived exosomal microRNAs shape the gut microbiota. *Cell Host Microbe* **24**, 637–652.e8 (2018).
35. K. Koeppen *et al*., A novel mechanism of host-pathogen interaction through sRNA in bacterial outer membrane vesicles. *PLoS Pathog.* **12**, e1005672 (2016).
36. G. A. O'Toole, Microtiter dish biofilm formation assay. *J. Vis. Exp.* **47**, 2437 (2011).
37. S. R. Baglio *et al*., Human bone marrow- and adipose-mesenchymal stem cells secrete exosomes enriched in distinctive miRNA and tRNA species. *Stem Cell Res. Ther.* **6**, 127 (2015).
38. L. Vojtech *et al*., Exosomes in human semen carry a distinctive repertoire of small non-coding RNAs with potential regulatory functions. *Nucleic Acids Res.* **42**, 7290–7304 (2014).
39. C. Quek *et al*., Defining the purity of exosomes required for diagnostic profiling of small RNA suitable for biomarker discovery. *RNA Biol.* **14**, 245–258 (2017).
40. M. R. Garcia-Silva, F. Cabrera-Cabrera, M. C. Güida, A. Cayota, Hints of tRNA-derived small RNAs role in RNA silencing mechanisms. *Genes (Basel)* **3**, 603–614 (2012).
41. Y. S. Lee, Y. Shibata, A. Malhotra, A. Dutta, A novel class of small RNAs: tRNA-derived RNA fragments (tRFs). *Genes Dev.* **23**, 2639–2649 (2009).
42. P. Kumar, J. Anaya, S. B. Mudunuri, A. Dutta, Meta-analysis of tRNA derived RNA fragments reveals that they are evolutionarily conserved and associate with AGO proteins to recognize specific RNA targets. *BMC Biol.* **12**, 78 (2014).
43. A. Busch, A. S. Richter, R. Backofen, IntaRNA: Efficient prediction of bacterial sRNA targets incorporating target site accessibility and seed regions. *Bioinformatics* **24**, 2849–2856 (2008).
44. S. Moreau-Marquis *et al*., The DeltaF508-CFTR mutation results in increased biofilm formation by *Pseudomonas aeruginosa* by increasing iron availability. *Am. J. Physiol. Lung Cell. Mol. Physiol.* **295**, L25–L37 (2008).
45. S. Moreau-Marquis, C. V. Redelman, B. A. Stanton, G. G. Anderson, Co-culture models of *Pseudomonas aeruginosa* biofilms grown on live human airway cells. *J. Vis. Exp.* **44**, 2186 (2010).
46. G. G. Anderson, S. Moreau-Marquis, B. A. Stanton, G. A. O'Toole, In vitro analysis of tobramycin-treated *Pseudomonas aeruginosa* biofilms on cystic fibrosis-derived airway epithelial cells. *Infect. Immun.* **76**, 1423–1433 (2008).
47. D. M. Cornforth, F. L. Diggle, J. A. Melvin, J. M. Bomberger, M. Whiteley, Quantitative framework for model evaluation in microbiology research using *Pseudomonas aeruginosa* and cystic fibrosis infection as a test case. *MBio* **11**, e03042-19 (2020).
48. B. P. Alcock *et al*., CARD 2020: Antibiotic resistome surveillance with the comprehensive antibiotic resistance database. *Nucleic Acids Res.* **48**, D517–D525 (2020).
49. M. Kanehisa, S. Goto, KEGG: Kyoto encyclopedia of genes and genomes. *Nucleic Acids Res.* **28**, 27–30 (2000).
50. J. Soria-Bustos *et al*., Two type VI secretion systems of *Enterobacter cloacae* are required for bacterial competition, cell adherence, and intestinal colonization. *Front. Microbiol.* **11**, 560488 (2020).
51. Y. Li, L. Chen, P. Zhang, A. Y. Bhagirath, K. Duan, ClpV3 of the H3-type VI secretion system (H3-T6SS) affects multiple virulence factors in *Pseudomonas aeruginosa*. *Front. Microbiol.* **11**, 1096 (2020).
52. J. Pan *et al*., Serine/threonine protein kinase PpkA contributes to the adaptation and virulence in *Pseudomonas aeruginosa*. *Microb. Pathog.* **113**, 5–10 (2017).
53. L. Chen, Y. Zou, A. A. Kronfl, Y. Wu, Type VI secretion system of *Pseudomonas aeruginosa* is associated with biofilm formation but not environmental adaptation. *MicrobiologyOpen* **9**, e991 (2020).
54. M. R. Hendricks *et al*., Extracellular vesicles promote transkingdom nutrient transfer during viral-bacterial co-infection. *Cell Rep.* **34**, 108672 (2021).
55. M. M. Shi *et al*., Role of miR-466 in mesenchymal stromal cell derived extracellular vesicles treating inoculation pneumonia caused by multidrug-resistant *Pseudomonas aeruginosa*. *Clin. Transl. Med.* **11**, e287 (2021).
56. S. F. Vencken, C. M. Greene, Toll-like receptors in cystic fibrosis: Impact of dysfunctional microRNA on innate immune responses in the cystic fibrosis lung. *J. Innate Immun.* **8**, 541–549 (2016).
57. L. R. Stolzenburg, A. Harris, The role of microRNAs in chronic respiratory disease: Recent insights. *Biol. Chem.* **399**, 219–234 (2018).
58. I. K. Oglesby *et al*., miR-17 overexpression in cystic fibrosis airway epithelial cells decreases interleukin-8 production. *Eur. Respir. J.* **46**, 1350–1360 (2015).
59. L. Y. Zhou, Z. Qin, Y. H. Zhu, Z. Y. He, T. Xu, Current RNA-based therapeutics in clinical trials. *Curr. Gene Ther.* **19**, 172–196 (2019).
60. C. de la Fuente-Núñez, F. Reffuveille, K. E. Fairfull-Smith, R. E. Hancock, Effect of nitroxides on swarming motility and biofilm formation, multicellular behaviors in *Pseudomonas aeruginosa*. *Antimicrob. Agents Chemother.* **57**, 4877–4881 (2013).
61. D. Kang, N. V. Kirienko, Interdependence between iron acquisition and biofilm formation in *Pseudomonas aeruginosa*. *J. Microbiol.* **56**, 449–457 (2018).
62. L. B. Rice, Mechanisms of resistance and clinical relevance of resistance to β-lactams, glycopeptides, and fluoroquinolones. *Mayo Clin. Proc.* **87**, 198–208 (2012).
63. T. J. Kidd *et al*.; Antimicrobial Resistance in Cystic Fibrosis International Working Group, Defining antimicrobial resistance in cystic fibrosis. *J. Cyst. Fibros.* **17**, 696–704 (2018).
64. S. A. Riquelme, D. Ahn, A. Prince, *Pseudomonas aeruginosa* and *Klebsiella pneumoniae* adaptation to innate immune clearance mechanisms in the lung. *J. Innate Immun.* **10**, 442–454 (2018).
65. D. Parker, D. Ahn, T. Cohen, A. Prince, Innate immune signaling activated by MDR bacteria in the airway. *Physiol. Rev.* **96**, 19–53 (2016).
66. S. Moreau-Marquis, B. Coutermarsh, B. A. Stanton, Combination of hypothiocyanite and lactoferrin (ALX-109) enhances the ability of tobramycin and aztreonam to eliminate *Pseudomonas aeruginosa* biofilms growing on cystic fibrosis airway epithelial cells. *J. Antimicrob. Chemother.* **70**, 160–166 (2015).

67. Q. Yu *et al*., In vitro evaluation of tobramycin and aztreonam versus *Pseudomonas aeruginosa* biofilms on cystic fibrosis-derived human airway epithelial cells. *J. Antimicrob. Chemother.* **67**, 2673–2681 (2012).
68. R. M. Shanks, N. C. Caiazza, S. M. Hinsa, C. M. Toutain, G. A. O'Toole, Saccharomyces cerevisiae-based molecular tool kit for manipulation of genes from gram-negative bacteria. *Appl. Environ. Microbiol.* **72**, 5027–5036 (2006).
69. T. H. Hampton, K. Koeppen, L. Bashor, B. A. Stanton, Selection of reference genes for quantitative PCR: Identifying reference genes for airway epithelial cells exposed to *Pseudomonas aeruginosa*. *Am. J. Physiol. Lung Cell. Mol. Physiol.* **319**, L256–L265 (2020).
70. R. Barnaby, K. Koeppen, B. A. Stanton, Cyclodextrins reduce the ability of *Pseudomonas aeruginosa* outer-membrane vesicles to reduce CFTR Cl^- secretion. *Am. J. Physiol. Lung Cell. Mol. Physiol.* **316**, L206–L215 (2019).
71. R. J. Lambert, J. Pearson, Susceptibility testing: Accurate and reproducible minimum inhibitory concentration (MIC) and non-inhibitory concentration (NIC) values. *J. Appl. Microbiol.* **88**, 784–790 (2000).
72. A. A. Malek, M. J. Wargo, D. A. Hogan, Absence of membrane phosphatidylcholine does not affect virulence and stress tolerance phenotypes in the opportunistic pathogen *Pseudomonas aeruginosa*. *PLoS One* **7**, e30829 (2012).
73. S. Moreau-Marquis, G. A. O'Toole, B. A. Stanton, Tobramycin and FDA-approved iron chelators eliminate *Pseudomonas aeruginosa* biofilms on cystic fibrosis cells. *Am. J. Respir. Cell Mol. Biol.* **41**, 305–313 (2009).
74. J. M. Bomberger *et al*., Long-distance delivery of bacterial virulence factors by *Pseudomonas aeruginosa* outer membrane vesicles. *PLoS Pathog.* **5**, e1000382 (2009).
75. A. Guha, A. Choudhury, B. G. Unni, M. K. Roy, Effect of outer-membrane permeabilizers on the activity of antibiotics and plant extracts against *Pseudomonas aeruginosa*. *Folia Microbiol. (Praha)* **47**, 379–384 (2002).
76. Y. Briers, M. Walmagh, R. Lavigne, Use of bacteriophage endolysin EL188 and outer membrane permeabilizers against *Pseudomonas aeruginosa*. *J. Appl. Microbiol.* **110**, 778–785 (2011).
77. R Core Team, R: A language and environment for statistical computing. R Foundation for Statistical Computing, Vienna, Austria (2021). https://www.R-project.org/.
78. H. Wickham, *ggplot2: Elegant Graphics for Data Analysis* (Springer International Publishing, New York, NY, ed. 2, 2016), p. 260.
79. D. Tenenbaum, *KEGGREST: Client-Side REST Access to KEGG. R Package Version 1.28.0* (2020).
80. M. Kanehisa *et al*., KEGG for linking genomes to life and the environment. *Nucleic Acids Res.* **36**, D480–D484 (2008).
81. B. C. Goodale *et al*., Profiling microRNA expression in Atlantic killifish (*Fundulus heteroclitus*) gill and responses to arsenic and hyperosmotic stress. *Aquat. Toxicol.* **206**, 142–153 (2019).
82. J. Pinheiro, D. Bates, S. DebRoy, D. Sarkar; R Core Team, *nlme: Linear and Nonlinear Mixed Effects Models* (2021).